D95-32
10P

N87-10514

18979

8.1.2 IMPROVING RANGE RESOLUTION WITH A FREQUENCY-HOPPING TECHNIQUE

G. R. Stitt and S. A. Bowhill

Aeronomy Laboratory
Department of Electrical and Computer Engineering
University of Illinois
Urbana, Illinois 61801

IB 647432

INTRODUCTION

Range resolution of a conventional pulsed Doppler radar is determined by the scattering volume defined by the transmitted pulse shape p(z). To increase the resolution, the length of the pulse must be reduced. Reducing the pulse length, however, also reduces the transmitted power and hence the signal-to-noise ratio unless the peak power capability of the transmitter is greatly increased, which is a very expensive process. Improved range resolution may also be attained through the use of various pulse-coding methods, but such methods are sometimes difficult to implement from a hardware standpoint. The "frequency-hopping" (F-H) technique to be described increases the range resolution of pulsed Doppler MST radar without the need for extensive modifications to the radar transmitter. This technique consists of sending a repeated sequence of pulses, each pulse in the sequence being transmitted at a unique radio frequency that is under the control of a microcomputer.

All of the radar parameters in the following discussion, such as pulsewidth and Inter Pulse Period (IPP), apply to the F-H system being developed for the Urbana radar.

ANALYSIS OF SYSTEM

Figure 1 shows one way of representing the pulse train sent by the radar transmitter. Since the wavelength of each pulse differs from that of its neighbors by about one centimeter, it is to be expected that echoes from a turbulent scatterer will differ slightly from each other in phase. Taking advantage of these phase differences constitutes the crux of the frequency-hopping technique.

The frequency sequence applied to consecutive transmitter pulses is also shown in the pulse pattern diagram of Figure 2. For example, at time t = 0, a pulse is sent at frequency ω_o; at time $t = \tau$, a pulse is sent at frequency $\omega_o + \Delta\omega$, and so forth. At time $t = 16\tau$, the pattern repeats itself. The range of frequencies covered by the pattern is 750 kHz, with contiguous frequencies separated by 50 kHz. Notice that the sawtooth waveform of Figure 2 repeats itself three times every 1/8 s. The present Urbana coherent scatter system integrates samples for 1/8 s. Hence, by integrating samples corresponding to three of the waveforms in Figure 2, the F-H system possesses a coherently integrated sample length identical to that of the present coherent scatter system. It must be realized, however, that only samples taken at the same frequency may be coherently summed. Consequently, each 1/8-second coherently integrated F-H sample actually consists of 16 subsamples, with each subsample comprised of three individual samples at the same frequency added together.

Consider the situation that the atmosphere contains only a single infinitely thin, mirror type scatterer located somewhere within the range gate z_o, and moving with a constant velocity v_d throughout the collection of a 1/8-second coherently integrated data sample. In this case, nonzero samples are obtained only for range gate z_o. Consider also the following sample sequence x(n):

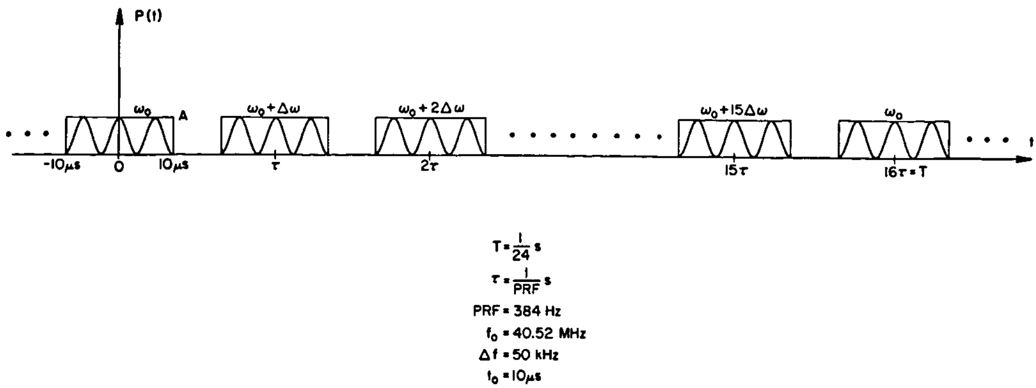

Figure 1. Pulse train sent by the radar.

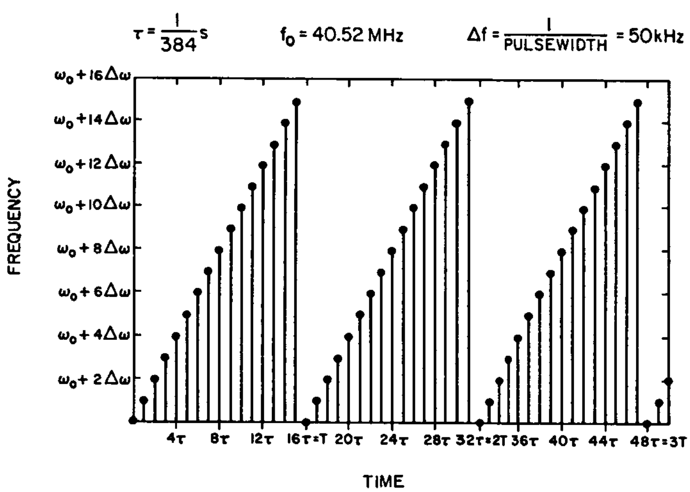

Figure 2. Time vs. frequency pulse pattern of the F-H system.

$$x(n) = B_n e^{j\phi_n} \tag{1}$$

where n = 0, 1, 2, ..., 47. x(n) is the sequence that results from sampling the radar returns caused by the reflection of the transmitted pulse train shown in Figure 1 from the mirror scatterer. Notice that the index of x(n) takes on the values 0-47. Hence, x(n) consists of all the individual samples contained in a single 1/8-second coherently integrated F-H sample. B_n is the magnitude of sample n, and ϕ_n is the phase.

The mirror scatterer is a delta function in range space; that is, as a function of z. Consequently, its Fourier transform is a constant for all values of wave number k. Since radar pulses are scattered by fluctuations in the index of refraction with a nonzero Fourier component equal to one-half the radar wavelength in the direction of propagation of the pulse, the ideal mirror scatterer reflects radar pulses at all frequencies equally well. As a result, all samples of the sequence x(n) have the same magnitude, and equation (1) may be rewritten as

$$x(n) = Be^{j\phi_n} \tag{2}$$

In order to consider the phase ϕ_n of the samples of the sequence x(n), it is convenient to make the following definitions. Let

τ = 1/384 s
f_o = 40.52 MHz
Δf = 50 kHz
v_d = the velocity of the scatterer
Δz = the distance, at time t = 0, at which the scatterer is located above or below z_o. Δz must satisfy the relation $|\Delta z| \leq 1.5$ km
λ_n = the wavelength of the nth radar pulse
f_n = the frequency of the nth radar pulse
$= f_o + (n)_{16}\Delta f$
z_n = the height of the scatterer when it reflects the nth radar pulse
$\approx z_o + \Delta z + v_d n\tau$
$(n)_{16}$ = n mod 16

With these definitions, ϕ_n may be written as

$$\begin{aligned}\phi_n &= \frac{4\pi}{\lambda_n} z_n \\ &= \frac{4\pi}{C}\left[f_o z_o + f_o\Delta z + f_o v_d n\tau + (n)_{16}\Delta f z_o + (n)_{16}\Delta f(\Delta z + v_d n\tau)\right]\end{aligned} \tag{3}$$

Substituting the above result for ϕ_n into equation (2) yields

$$x_n = B\exp\{j\frac{4\pi}{C}[f_o z_o + f_o\Delta z + f_o v_d n\tau + (n)_{16}\Delta f z_o + (n)_{16}\Delta f(\Delta z + v_d n\tau)]\}$$

Let us define the constant α as

$$\alpha = \frac{4\pi}{C}(f_o z_o + f_o\Delta z)$$

Using this definition, and noting the property

$$\exp\{j\frac{4\pi}{C}[(n)_{16}\Delta f z_o]\} = 1$$

the expression for x(n) may be written as

$$x(n) = Be^{j\alpha}\exp\{j\frac{4\pi}{C}[f_o v_d n\tau + (n)_{16}\Delta f(\Delta z + v_d n\tau)]\} \tag{4}$$

Recall that in each 1/8-second coherently integrated F-H sample, individual samples at the same frequency are to be coherently summed. So if y(n) is the 16-point sequence that results from adding individual samples at the same frequency, then

$$y(n) = \sum_{m=0}^{2} x(16m+n)$$

$$\approx 3B \exp\{j\frac{4\pi}{C}[f_o z_o + \Delta z(f_o + n\Delta f) + v_d(16\tau + n\tau)(f_o + n\Delta f)]\} \qquad (5)$$

where n = 0, 1,..., 15. Notice that since the index of the sequence y(n) has a maximum value of 15, the clumsy modular notation has been dropped.

The third phase term in equation (5) results in a systematic error in the range estimation of the scatterer, due to the velocity of the scatterer itself. However, this effect is of concern only if the third phase term is approximately the same size as the second, which is due to the actual position of the scatterer. In order to gain an idea of the scatterer velocity that is necessary for this to occur, the two terms may be set equal.

$$v_d = \frac{\Delta z}{16\tau + n\tau}$$

Substituting the worst case values Δz = 200m, n = 15 into the equation above, it becomes clear that the scatterer must be moving with a velocity of at least v_d = 2500 m/s in order for the two terms to be about equal. Hence, for all practical purposes, the third phase term of equation (5) may be ignored.

Recalling the definition of α, a constant D may be defined as D = 3B exp($j\alpha$). Using this definition and the equation

$$\frac{4\pi}{C}\ (n\Delta f\Delta z) = \frac{n\pi\Delta z}{8d_o}$$

where d_o = 187.5 m, equation (5) may be rewritten as

$$y(n) = D \exp(j\frac{n\pi\Delta z}{8d_o}) \qquad (6)$$

where n = 0, 1, ..., 15.

Equation (6) reveals the form of the individual samples in a single 1/8-second coherently integrated F-H sample, assuming a single mirror-type scatterer located somewhere within the range gate z_o. As anticipated, each sample has the same magnitude, and there is a phase difference from one sample to the next. This intersample phase difference is in fact linear, and its size depends upon the distance Δz of the scatterer from the center of the scattering volume (z_o).

To take advantage of the linear intersample phase shift present in the sequence y(n) of equation (6), it is possible to simply calculate the DFT of the sequence. Figure 3 shows graphs of the sequence Y(p) resulting from the DFT of y(n), assuming different values for Δz. It is clear that as Δz becomes more positive, the intersample phase shift in (6) becomes larger, and the central peak of Y(p) moves up the graph. Conversely, as Δz becomes more and more negative, the central peak of Y(p) wraps around to the top of the graph, and begins to move down it.

When a 1/8-second coherently integrated F-H sample is obtained from the atmosphere for range gate z_o, the value of Δz is of course not known. It is made clear by the graphs of Figure 3, however, that by taking the DFT of the individual samples within the coherently integrated sample, it is possible to deduce the position of the scatterer Δz within the scattering volume by the position of the central peak of Y(p). This fact is the basis for the improved range resolution offered by the frequency-hopping technique.

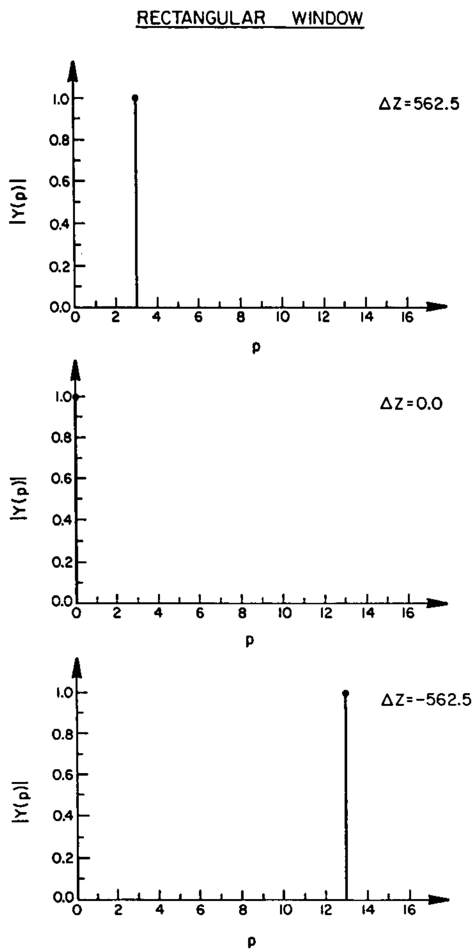

Figure 3. Y(p) for different values of Δz.

A more complex analysis involving the convolution of the pulse train in Figure 1 with scatterers present in the atmosphere, and taking into account the coherent detection scheme employed by the Urbana radar, has also been performed; it yields results similar to those obtained using the more intuitive approach outlined above.

COMPLICATIONS IN ANALYSIS

All of the values of Δz assumed in the graphs of Figure 3 are integer multiples of d_o = 187.5 m. d_o is the basic range resolution of the frequency-hopping system; integer multiples of d_o may therefore be termed "subrange" gates of the system. Hence, all of the scatterers in the graphs of Figure 3 are assumed to fall exactly in the middle of a subrange gate. This pleasant situation is unlikely to be duplicated in the real atmosphere. Figures 4(a) and 5(a) show graphs of Y(p) plotted in semilog form for more arbitrary values of Δz. A scatterer is shown starting in the middle of the third subrange gate, and gradually moving downward until it reaches the point

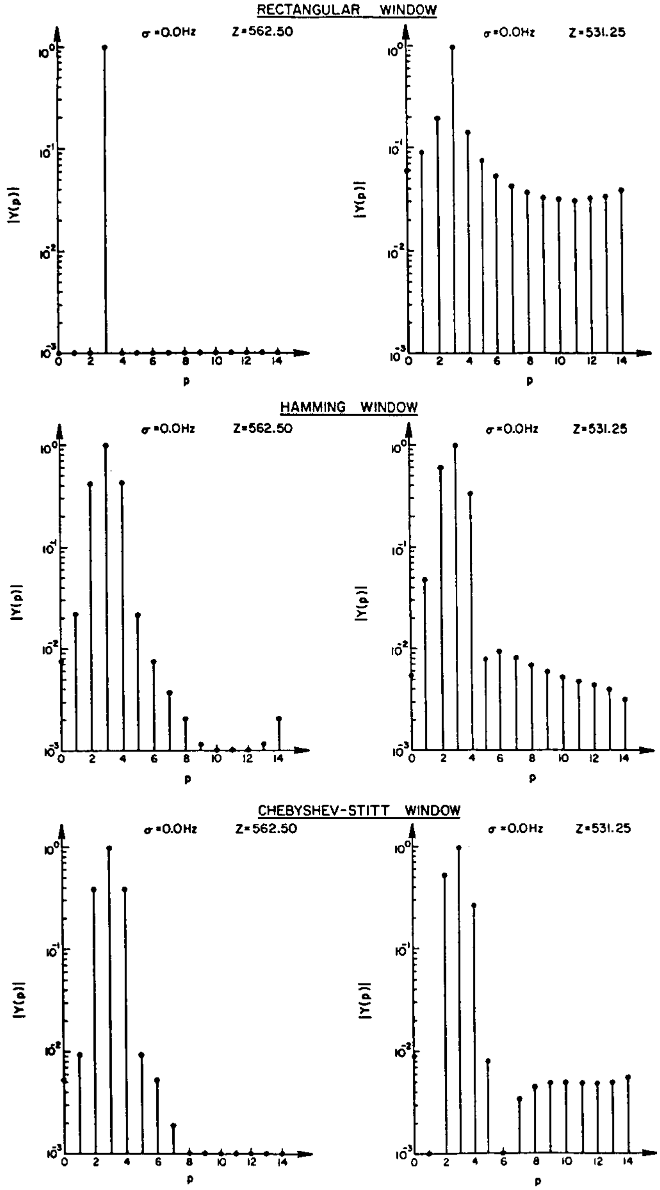

Figure 4. Effects of different windows.

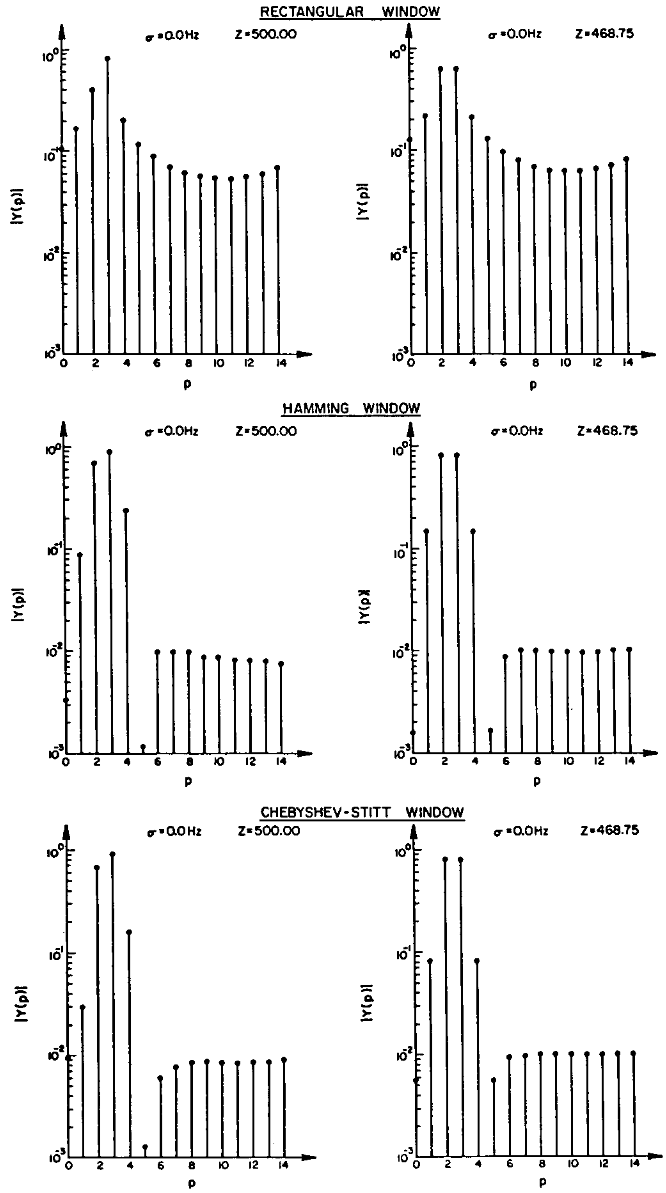

Figure 5. Effects of different windows.

halfway between the second and third subrange gates. The central peak of Y(p) remains in the correct position, but it is now accompanied by undesirable sidelobes in the subrange gates that should be zero.

The sidelobes present in the graphs of Figures 4(a) and 5(a) are due to the fact that the sequence y(n) of equation (6) is unwindowed; or, to be more precise, a rectangular window has been applied. To reduce the sidelobes, a window having more gently rounded edges may be used. In other words, we may derive a new sequence y(n), having more desirable transform properties, from the old sequence y(n) as follows

$$y(n) = Dn \exp(j\frac{n\pi\Delta z}{8d_o}) \tag{7}$$

where $D_n = w(n)D$, and w(n) is a windowing sequence of length 16.

Figures 4(b) and 5(b) show the effects of selecting a Hamming window sequence for w(n). A useful reduction in sidelobe level has been achieved, at the cost of a slight increase in the width of the main peak, or lobe, of the sequence Y(p).

Although the standard Hamming window quite effectively reduces the sidelobes of Y(p), the unusual form of the sequence y(n) in equation (7) makes possible a somewhat more clever approach. Since the weighting sequence D_n in (7) is arbitrary, it is possible to specify that D_n must be symmetric about its center. In this case, it may be shown that the DFT of y(n) can be written as

$$Y(\psi) = \sum_{n=0}^{\frac{N}{2}-1} An \cos[(2n+1)\frac{\psi}{2}] \tag{8}$$

where
$$A_n = A_{-(n+1)}$$
$$= D_{n+N/2}$$
$$\Psi = \pi(p - \Delta z/d_o)/8$$
$$N = 16$$

Since a relationship exists between A_n and D_n, if values can be found for A_n, then the values of the weighting coefficients D_n will be known. One way of finding appropriate values for A_n is by solving the equation

$$Y(\psi) = T_7(x)$$

where $T_7(x)$ = a seventh order Chebyshev polynomial (9)
$x = a \cos(\Psi/2)$
a = an arbitrary constant

$T_7(x)$ is a polynomial consisting of terms of the form $[a \cos(\Psi/2)]^k$, where k is an odd, positive integer. On the other hand, $Y(\Psi)$ is a polynomial consisting of terms of the form $\cos(p\,\Psi/2)$, where p is also an odd, positive integer. In order to solve equation (9), then, trigonometric identities must be used to reduce terms of the form $[a \cos(\Psi/2)]^k$ into terms of the form $\cos(p\,\Psi/2)$. This can be a very tedious process. Fortunately, operations of this kind are tabulated in books on antenna engineering (see, e.g, JASIK, 1961).

Figures 4(c) and 5(c) show the results of applying a window of this type to the sequence of equation (7). Although these results appear very similar to those obtained using a standard Hamming window, the sidelobe levels and mainlobe width have in fact been slightly reduced. A window of this type should be optimal in the sense of giving the narrowest possible main lobe for a specified sidelobe level, or vice versa. The main lobe width may be varied by adjusting the value of the arbitrary constant a. In generating the graphs of Figures 4(c) and 5(c), the value of a was chosen so that the sidelobe level is approximately 40 dB below the main lobe peak.

The Urbana radar normally employs a 20μs pulse, so that range gates are separated by 3.0 km intervals. When the F-H technique is employed, however, such range gate spacing can cause range-aliasing problems. In particular, when a scatterer is located at the boundary of two range gates, it becomes impossible to determine its correct position. By oversampling at 1.5 km intervals, it is possible to construct an unaliased vertical profile by throwing out the subrange gates at the edges of each range gate, then fitting the remaining subrange gates together in a manner analogous to the "overlap-save" algorithm used to perform large DFTs (see, e.g., OPPENHEIM and SCHAFER 1975).

SUMMARY OF DATA ANALYSIS PROCEDURE

At this point, a fairly thorough discussion has been given of the manner in which a single 1/8-second coherently integrated F-H sample might be processed. No mention has been made, however, of the way in which an entire minutes' worth of data for a single range gate is to be processed. Figure 6 shows one way of representing such a block of data. In order to understand the graph in this figure, it is perhaps easiest to make the following set of definitions:

$x(m,n)$ = a two-dimensional data sequence containing one minutes' worth of F-H data for a single range gate. Each column consists of a single 1/8-second coherently integrated F-H sample.

M = the number of 1/8-second coherently integrated samples in one minute of data.

N = the number of frequencies at which the F-H system operates. This number is 16 for the present system.

$t' = 1/8$ s.

mt' = the time at which the mth column is collected.

$f_o+n\Delta f$ = the transmitting frequency corresponding to the nth element of a column.

Assume that the range gate corresponding to the data of Figure 6 contains only one scatterer. Suppose that the one-dimensional DFT of the first column in Figure 6 is calculated. Earlier discussions suggest that only one element (or perhaps two) of the resulting column is essentially nonzero. Precisely which element is nonzero depends, of course, on the position of the scatterer within the scattering volume. Now suppose that the one-dimensional DFTs of all of the columns in Figure 6 are taken. After the completion of these operations, only one row of the resulting graph is essentially nonzero. The position of that row may be used to determine the position of the scatterer within the scattering volume. By taking the one-dimensional autocorrelation function of the nonzero row, the usual parameters of velocity, power, and correlation time may be derived for the single scatterer.

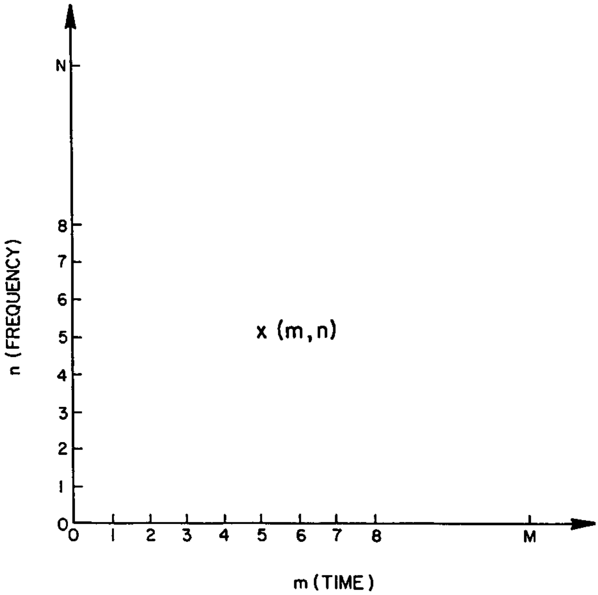

Figure 6. Representation for one minute of data in a single range gate of the F-H system.

Thus, a one-minute block of data, such as that represented in Figure 6, may be processed in five steps:

(1) Each column of the two-dimensional sequence is windowed using a Chebyshev window of the type discussed earlier.

(2) Each column of the sequence is transformed using a one-dimensional DFT.

(3) Undesired rows are thrown out using the overlap-save algorithm discussed earlier.

(4) The one-dimensional autocorrelation function of each of the remaining rows is found.

(5) The usual velocity, power, and correlation time parameters are derived for each row.

ACKNOWLEDGEMENT

The research described in this paper was supported by the National Aeronautics and Space Administration under Grant NSG 7506.

REFERENCES

Jasik, H. (1961), Editor, Antenna Engineering Handbook, Mcgraw-Hill, NY.

Oppenheim, A. V. and R. W. Schafer (1975), Digital Signal Processing, Prentice-Hall, NJ.